Journal of Sound and Vibration 417 (2018) 19–37

Contents lists available at ScienceDirect

Journal of Sound and Vibration

journal homepage: www.elsevier.com/locate/jsvi

The level crossing rates and associated statistical properties of a random frequency response function

Robin S. Langley

Department of Engineering, University of Cambridge, Trumpington Street, Cambridge CB2 1PZ, UK

ARTICLE INFO

Article history:
Received 28 June 2017
Received in revised form 28 November 2017
Accepted 1 December 2017
Available online 6 December 2017

Keywords:
Random systems
Frequency response functions
Linear vibration
Random vibration

ABSTRACT

This work is concerned with the statistical properties of the frequency response function of the energy of a random system. Earlier studies have considered the statistical distribution of the function at a single frequency, or alternatively the statistics of a band-average of the function. In contrast the present analysis considers the statistical fluctuations over a frequency band, and results are obtained for the mean rate at which the function crosses a specified level (or equivalently, the average number of times the level is crossed within the band). Results are also obtained for the probability of crossing a specified level at least once, the mean rate of occurrence of peaks, and the mean trough-to-peak height. The analysis is based on the assumption that the natural frequencies and mode shapes of the system have statistical properties that are governed by the Gaussian Orthogonal Ensemble (GOE), and the validity of this assumption is demonstrated by comparison with numerical simulations for a random plate. The work has application to the assessment of the performance of dynamic systems that are sensitive to random imperfections.

1. Introduction

The prediction of the response of a linear system to harmonic forcing is straight forward in principle: the governing equations of most system components are well established, and highly sophisticated computer software is widely available to provide numerical solutions to these equations. A difficulty arises however if the system properties are random or otherwise uncertain, since this requires the uncertainty to be quantified and then propagated through the system equations of motion to yield the uncertainty in the response. Both aspects of this procedure are problematical – firstly it can be difficult or impossible to fully identify and quantify the system uncertainties (for example, in terms of probability density functions, or bounded variables), and secondly the propagation of the uncertainty can require very significant computational resources. For these reasons there is considerable interest in alternative methods of predicting the uncertainty in the harmonic response of an uncertain linear system, and in fact this has been a topic of research for more than half a century.

Early progress in predicting the response statistics of complex systems was made in the field of room acoustics by Schroeder and his co-workers. By 1954 expressions had been derived for a number of important statistical properties of the frequency response function (FRF) of the pressure in a room, including the mean value of the trough-to-peak height and the mean spacing between peaks [1,2]. It was assumed on the basis of the Central Limit Theorem (CLT) that the pressure has a complex-Gaussian distribution, and further work along these lines then considered the frequency-correlation function of the pressure FRF [3]. The application of the CLT rests on the assumption that many modes contribute to the response at any one

E-mail address: rsl21@eng.cam.ac.uk.

https://doi.org/10.1016/j.jsv.2017.12.001

frequency, and this requires a parameter known as the modal overlap to be high (typically greater than 3). The frequency beyond which this condition is met is known as the Schroeder frequency. In practice there is considerable interest in the statistical properties of an FRF below the Schroeder frequency, and later authors have considered this problem. In 1969 Lyon [4] developed a theory for the variance of the power input to a random structural or acoustic system, based initially on the premise that the system natural frequencies form a Poisson point process, but then with some allowance for effect of "repulsion" between natural frequencies. Lyon and his co-workers later considered the statistics of the phase of an FRF, and in particular the way in which the poles and zeros of the FRF affect the mean phase progression (for example [5,6]). Research in random matrix theory [7] throughout the 1970s and 1980s led to the realisation that the modal statistics of a highly random dynamic system might obey a universal distribution, and this fact was highlighted in 1989 by Weaver [8]. The universal distribution is known as the Gaussian Orthogonal Ensemble (GOE), with the name arising from a particular type of random matrix that is amenable to the derivation of closed-form eigenvalue statistics [7]. Much subsequent work on the topic of random FRFs has exploited the occurrence of GOE statistics [9], and expressions are available (for example) for the variance of both the frequency response [10,11] and the band-averaged response [12] of system components. The approach has also been combined with Statistical Energy Analysis (SEA) methods to yield the variance of the response of complex built-up systems [13,14]. As described below, the aim of the present work is to extend existing results to further properties of a random FRF. For completeness, it should be noted that the occurrence of GOE statistics requires the system to be sufficiently random, and if this is not the case then parametric uncertainties (for example [15]) may need to be considered, or alternatively the maximum entropy approach developed by Soize [16] might be applied. The present work is exclusively concerned with systems that might reasonably be assumed to display GOE statistics.

Previous work on the application of the GOE to FRF statistics has tended to focus on the prediction of the mean and variance, and ultimately the probability density function, of the response at a single frequency. This enables the probability that the response will exceed a particular level at a given frequency to be estimated, and confidence bands for the response can be established [17]. More general statistical questions that cannot be answered by using "single frequency" statistics include: (i) the probability that the FRF will exceed a particular level at least once within a given frequency band, and (ii) the average number of crossings of a particular level within a given frequency band. These questions would be of practical interest, for example, if the frequency of excitation is uncertain but known to lie within a particular band. These questions are addressed in the present work for the case of the FRF of the energy of a random system, and related questions such as the mean rate of the occurrence of peaks, and the mean trough-to-peak height are also addressed. The work makes extensive use of previous results from the random vibration literature concerning the mean rate at which a random process crosses a critical level [18]; this requires a new result to be derived for the variance of the slope (i.e. the frequency derivative) of the FRF and also for the *conditional* variance of the slope, meaning the variance at a prescribed value of the FRF. The prediction of the mean rate of the occurrence of peaks, and the mean trough-to-peak height, requires knowledge of the variance of the second derivative of the FRF, and again a new result is derived here for this quantity.

Section 2 of what follows presents background material regarding the FRF of the energy of a random system; the mean rate at which this function crosses a specified level is then derived in Section 3. Various other statistical properties of the function are then derived in Section 4, namely: the probability of crossing a specified level at least once, the mean rate of the occurrence of peaks, and the mean trough-to-peak height. The theoretical results are then compared in Section 5 with numerical results for a random plate.

2. Random frequency response functions

If a structural dynamic system is subjected harmonic forcing at frequency ω and has proportional damping (or if the damping can be reasonably approximated as being proportional) then the complex amplitude of a displacement response u at some location $\mathbf{x}$ within the system can be written in the well-known form [19].

$$u(\omega,\mathbf{x}) = \sum_n \frac{i\omega\, g_n \phi_n(\mathbf{x})}{\omega_n^2 - \omega^2 + i\eta\omega_n^2}, \quad g_n = \int_R P(\mathbf{x})\phi_n(\mathbf{x})\mathrm{d}\mathbf{x}. \tag{1,2}$$

Here ω_n is the nth natural frequency of the system, ϕ_n is the associated mode shape (scaled to unit generalised mass), and $P(\mathbf{x})$ describes the spatial distribution of the applied loading so that g_n is the generalised force acting in the nth mode. The time averaged kinetic energy of the system can be written as

$$T(\omega) = (1/4)\int_R \rho(\mathbf{x})|u(\omega,\mathbf{x})|^2\mathrm{d}\mathbf{x}, \tag{3}$$

where $\rho(\mathbf{x})$ is the mass density and R is the spatial region occupied by the system. For ease of notation Eqs. (1)–(3) are explicitly concerned with the case of a scalar displacement variable and scalar mode shapes, although these results could readily be generalised to the case of vector quantities if required. It follows from Eqs. (1)–(3), and the fact that the mode shapes are mass-orthogonal, that the kinetic energy of the system can be written in the form

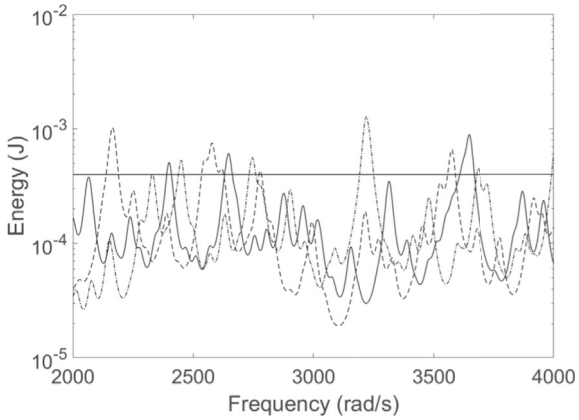

Fig. 1. Three realizations of the energy response of a plate with randomly placed masses. The horizontal line represents a level b, and the interest is in the number of times this level is crossed by the energy. The properties of the plate are given in the text.

$$T(\omega) = \sum_n a_n H(\omega, \omega_n), \tag{4}$$

where

$$a_n = |g_n|^2, \quad H(\omega, \omega_n) = \frac{\left(\omega^2/4\right)}{\left(\omega_n^2 - \omega^2\right)^2 + \left(\eta\omega_n^2\right)^2}. \tag{5,6}$$

The present work is concerned with the statistical properties of the kinetic energy over an ensemble of random systems. In practice the randomness in a complex system may arise from manufacturing and assembly uncertainties, and an illustration of the typical effect on the system response can be afforded by a very simple example of a plate that has a number of masses attached at random locations. The natural frequencies and mode shapes of the system will differ for each arrangement of the masses, and the function $T(\omega)$ will therefore vary randomly across the ensemble of possible arrangements. An example of this is shown in Fig. 1 for a simply supported steel plate of thickness 1 mm and planform dimensions 0.8m $\times$ 0.67m, with 10 masses attached in random positions, each having 2% of the mass of the bare plate. The response of the system to a harmonic point force of amplitude $\sqrt{2}$ N has been calculated using the Lagrange-Rayleigh-Ritz approach [19], and the computed kinetic energy is shown as a function of frequency over the range 2000 rad/s to 4000 rad/s for three different arrangements of the masses. The modal density of the system (i.e. the average number of modes in a unit frequency band) is $n = 0.0278$, meaning that there are around 55 modes in the frequency band under consideration, and a frequency dependent loss factor in the form $\eta = 0.0179 \times (2000/\omega)$ has been employed, so that the modal overlap factor (defined as $m = \omega\eta n$) is unity across the whole frequency range. It can be seen in the figure that there is considerable random variation in the response of the system. The statistics of the response at a single frequency, and the statistics of frequency-band-averaged measures of the response, have each been the subject of much previous research [8–12]. The present work is concerned with a different issue, namely the average number of times the energy crosses a critical level within a specified frequency band, and the related problem of the probability that the energy will cross the critical level at least once in the frequency band. This issue is illustrated in Fig. 1, where the indicated response level is crossed at random positions by the different response curves, and it can readily be imagined that the probability of crossing at least once will reduce significantly as the level is increased. It is shown in the following section that closed form expressions can be obtained for both the mean rate of crossing the level and the probability of crossing the level at least once. Although the example of a random plate has been introduced to focus ideas, the following analysis is generally applicable to any system that displays a sufficient degree of randomness in a sense that is described below (in Section 3.2).

3. Crossing rates

3.1. General formulation

The solution to the problem of predicting the mean rate at which a stochastic process $y(t)$ crosses a prescribed level has long been established in the literature relating to random processes and random vibration [18]. Rice [20] was the first to show that the mean rate ν_b^+ at which the process crosses a level b with positive slope (a so called "up-crossing") can be written in terms of the joint probability density function of the process and its velocity, $p(\dot{y}, y)$, in the form

$$\nu_b^+ = \int_0^\infty \dot{y} p(\dot{y}, b) \mathrm{d}\dot{y}. \tag{7}$$

This result can be applied immediately to the present problem by identifying $y(t)$ with $T(\omega)$ and introducing an effective "velocity" for the kinetic energy via the definition

$$s(\omega) = \frac{\partial T(\omega)}{\partial \omega}, \tag{8}$$

so that mean crossing rate for the kinetic energy can be written in terms of the joint probability density function $p(s, T)$ in the form

$$\nu_b^+ = \int_0^\infty s p(s, b) \mathrm{d}s. \tag{9}$$

Note that in general both the function $p(s, T)$ and the crossing rate ν_b^+ will be functions of ω, but for ease of notation this dependency is not expressed explicitly.

Given Eq. (9), the crossing rate problem is now reduced to finding $p(s, T)$ for the kinetic energy function defined by Eq. (4). Progress can be made by noting that under certain conditions the marginal distribution of the kinetic energy tends to be lognormal [21], so that

$$p(T) = \frac{1}{\sqrt{2\pi}(Tc_1)} \exp\left\{ -\frac{1}{2}\left(\frac{\ln T - c_2}{c_1}\right)^2 \right\}, \tag{10}$$

where

$$c_1 = \sqrt{\ln\left(1 + \sigma^2 / \mu^2\right)}, \quad c_2 = \ln\left(\frac{\mu}{\sqrt{1 + \sigma^2 / \mu^2}}\right), \tag{11,12}$$

and

$$\mu = \mathrm{E}[T], \quad \sigma^2 = \mathrm{Var}[T]. \tag{13,14}$$

The conditions required for Eq. (10) to apply, together with closed form expressions for σ and μ, are given in Section 3.2. For the present argument is is sufficient to note at this stage that $p(T)$ can be assumed to be known, and noting also that

$$p(s, T) = p(s|T) p(T), \tag{15}$$

then implies that the solution of the crossing rate problem reduces to finding an expression for the conditional probability density function $p(s|T)$. The analogous function for the random vibration problem is $p(\dot{y}|y)$; in that case the interest is usually in stationary Gaussian random processes, for which the displacement and velocity are statistically independent and $p(\dot{y}|y) = p(\dot{y})$ is a Gaussian distribution. It is tempting to assume that independence will also apply in the present case, and as a test of this hypothesis numerical results for $p(s, T)$ have been generated for the random plate considered in the previous section. These results are shown in Fig. 2 (for $\omega = 2000$ rad/s), and it is immediately obvious that there is a strong dependency between s and T; moreover, at a given value of T the distribution of s appears to be bounded, and the width of the bounds grows linearly with T. As discussed in what follows, this phenomena can be explained by considering the nature of the function $H(\omega, \omega_n)$ that appears in Eq. (4).

The kinetic energy is expressed in Eq. (4) as a sum of contributions from the system modes of vibration. The contribution from the nth mode, $a_n H(\omega, \omega_n)$, will generally be important only in the vicinity of resonance, $\omega \approx \omega_n$, and in this vicinity it is reasonable to make the approximation $\omega + \omega_n \approx 2\omega$ in the denominator of $H(\omega, \omega_n)$ to give

$$H(\omega, \omega_n) \approx \frac{(1/4)}{4(\omega_n - \omega)^2 + (\eta\omega_n)^2}. \tag{16}$$

The variable s is defined as the frequency derivative of T, and s can therefore be expressed as a sum of the frequency derivatives of the functions $H(\omega, \omega_n)$. Now it follows from Eq. (16) that

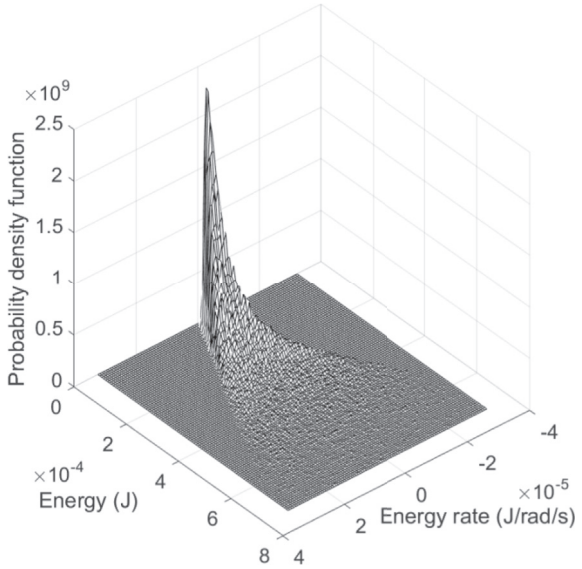

Fig. 2. The joint probability density function $p(s,T)$ of the energy and the energy rate (i.e. the frequency derivative of the energy) of a random plate at the frequency 2000 rad/s. The plate has the same properties as that considered in Fig. 1.

$$\frac{\partial H(\omega,\omega_n)}{\partial\omega}\approx\left[\frac{8(\omega_n-\omega)}{4(\omega_n-\omega)^2+(\eta\omega_n)^2}\right]H(\omega,\omega_n), \tag{17}$$

The maximum and minimum possible values of the term in the square brackets on the right of this expression can be shown to be $\pm 1/(\eta\omega_n)$, from which it follows that

$$\left|\frac{\partial H(\omega,\omega_n)}{\partial\omega}\right|\le\left(\frac{1}{\eta\omega_n}\right)H(\omega,\omega_n). \tag{18}$$

Now given that the coefficients a_n that appear in the series expansion of T are all positive, and that each term in the series makes a significant contribution in the vicinity of resonance, then Eqs. (4) and (18) imply that

$$|s|=\left|\frac{\partial T(\omega)}{\partial\omega}\right|\le\left(\frac{1}{\eta\omega}\right)T(\omega). \tag{19}$$

Clearly a number of approximations have been made in the derivation of Eq. (19), but nonetheless when plotted on a contour map of $p(s,T)$, as shown in Fig. 3, the bounds indicated by the equation are in very good agreement with the bounds observed in the numerical simulations. The slight asymmetry that can be seen in the numerical simulations is not picked up by the present theory, due to the use of the symmetric approximation represented by Eq. (16). A key point is that the bounds grow linearly with T, and a further question is whether the conditional standard deviation of s, $\sigma_{sc}(T)$ say, will also grow linearly with T. Numerical results for $\sigma_{sc}(T)$ for the random plate example are presented in Fig. 4 and, focussing on the two solid curves shown in the figure, it can be seen that a linear approximation is reasonable, particularly when T is not too small. If a linear approximation is adopted, then the conditional variance can be written in the form

$$\sigma_{sc}(T)=cT, \tag{20}$$

and the question arises as to whether an analytical expression can be found for the constant c. Progress can be made by noting that if s is taken to have zero mean, then the unconditional (marginal) variance can be written in the form

$$\sigma_s^2=\int_0^\infty\sigma_{sc}^2(T)p(T)\mathrm{d}T=c^2\left(\sigma^2+\mu^2\right), \tag{21}$$

from which it follows that

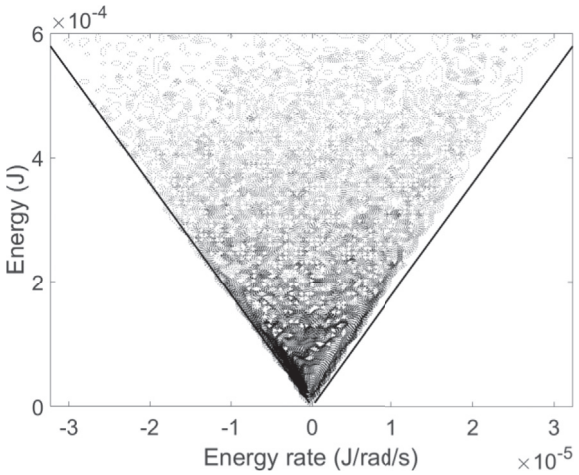

Fig. 3. Contour map of the joint probability density function of the energy and the energy rate of a random plate at the frequency 2000 rad/s. The two lines indicate the bounds on the rate predicted by Eq. (19). The plate has the same properties as that considered in Fig. 1.

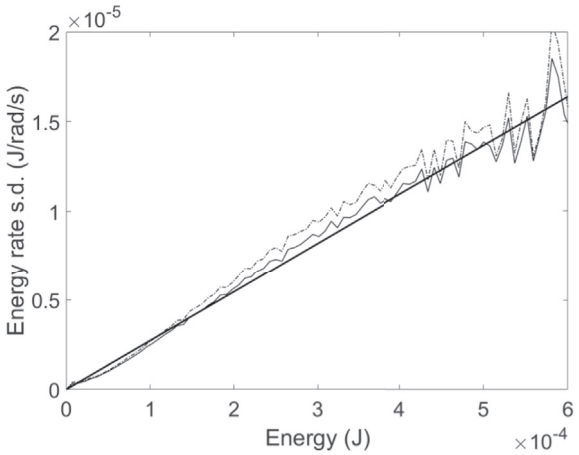

Fig. 4. The conditional standard deviation of the energy rate $\sigma_{sc}(T)$ plotted against the energy T, at the frequency 2000 rad/s. Solid irregular curve: numerical simulation of $\sigma_{sc}(T)$. Solid straight line: linear prediction of $\sigma_{sc}(T)$ given by Eq. (22). Chain dotted irregular curve: numerical results for the conditional mean value of the energy slope s, for positive s, divided by the value $\beta = 0.3989$ (this result would coincide with $\sigma_{sc}(T)$ were the energy rate to have a Gaussian distribution). The plate has the same properties as that considered in Fig. 1.

$$\sigma_{sc}(T) = \left(\sigma^2 + \mu^2\right)^{-1/2} \sigma_s T. \tag{22}$$

It is shown in Section 3.2 and the Appendix that a closed form expression for σ_s can be obtained, and thus Eq. (22) contains the required closed form expression for c; in fact, the linear approximation to $\sigma_{sc}(T)$ shown in Fig. 4 has been calculated using this equation. The fact that $\sigma_{sc}(T)$ is an increasing function of T can be explained physically by noting the asymmetry of the typical response curves shown in Fig. 1. The troughs of the curves tend to be broad while the peaks tend to be narrow, meaning that the rate of change is more likely to be large near to the higher values of the response.

Having derived an expression for the conditional variance of s, further progress can be made by noting that Eqs. (9) and (15) imply that the crossing rate can be expressed as

$$\nu_b^+ = p(b) \int_0^\infty s p(s|b) \mathrm{d}s. \tag{23}$$

The integral on the right hand side of this expression yields half the conditional mean value of s for positive s (as opposed to the mean value over both positive and negative values, which can be taken to be zero). Were the conditional distribution of

s Gaussian, then this integral would yield the value $\sigma_{sc}(b)/\sqrt{2\pi} = 0.3989\sigma_{sc}(b)$; were the conditional distribution exponential, then the result would be $\sigma_{sc}(b)/(2\sqrt{2}) = 0.3536\sigma_{sc}(b)$. It is therefore a reasonable approximation to write

$$\int_0^\infty sp(s|b)\mathrm{d}s = \beta\sigma_{sc}(b), \tag{24}$$

where β would take the values 0.3989 and 0.3536 for the two distributions mentioned earlier. Numerical results for the conditional mean value of s are shown in Fig. 4 for the plate example, and these results indicate that the Gaussian value of β yields a good approximation for this case. The adoption of Eq. (23) yields the following final result for the crossing rate

$$\nu_b^+ = \beta\sigma_s\left(\sigma^2 + \mu^2\right)^{-1/2} bp(b). \tag{25}$$

This result depends only on the level b, the constant β, and the three statistical parameters μ, σ, and σ_s. It is shown in the following section that closed form expressions can be obtained for each of these parameters. It should be noted that although a number of the approximations employed in the above analysis have been based on empirical evidence provided by the plate example, the validity of these approximations is not restricted to this type of example – the principle of universality (discussed below) implies that similar results would be obtained for all systems that are sufficiently random.

The average number of crossings that occur between two frequencies ω_A and ω_B can readily be computed from Eq. (25), although it should be noted that the crossing rate will in general be frequency dependent - this dependency can be expressed explicitly as $\nu_b^+(\omega)$. The number of crossings is then

$$N^+ = \int_{\omega_A}^{\omega_B} \nu_b^+(\omega)\mathrm{d}\omega. \tag{26}$$

3.2. The mean and variance parameters

The mean and variance of the kinetic energy, as defined by Eqs. (4), (13) and (14), will clearly depend on the statistics of the natural frequencies and mode shapes of the system. In general the statistical distributions of these quantities will depend in a complex way on the statistics of the system uncertainties, and hence it may initially be thought that little progress can be made in deriving general expressions for the parameters that are required in the crossing rate formula, Eq. (25). However, there is much empirical evidence to suggest that if a dynamic system has a sufficient degree of randomness and non-localised modes, then the statistical distribution of the natural frequencies and mode shapes conform to the Gaussian Orthogonal Ensemble (GOE) regardless of the detailed nature of the underlying uncertainty [9]. This "universal" behaviour tends to be observed when the statistical overlap factor of the system is greater than unity, meaning that the random shifts in the natural frequencies exceed the mean frequency spacing, so that there is a high degree of "mixing" of the modes across the ensemble, i.e. a reasonable number of the modes of one member of the ensemble are needed to represent a mode of a second member of the ensemble [22]. The GOE distribution for the natural frequencies depends on only one parameter, the modal density, and so very powerful results can be obtained from very little information about the system. The theoretical justification for the use of a lognormal distribution of kinetic energy, Eq. (10), also rests on the occurrence of GOE statistics – in Ref. [21] it is shown that this distribution emerges for a GOE system with a sufficient degree of modal overlap.

Previous work on GOE systems has led to expressions for the mean and variance of the kinetic energy (for example [23]). The result for the mean is

$$\mu = \frac{\mathrm{E}[a_n]\pi n(\omega)}{8\eta\omega}, \tag{27}$$

where $n(\omega)$ is the modal density. The modal density of standard structural components can be calculated using asymptotic methods [24], and the average value of the coefficient a_n can be obtained from the mode shape statistics associated with the GOE, so that all of the information required by Eq. (27) can readily be established. Likewise, previous research has shown that the variance of the energy is given by Ref. [25]:

$$\sigma^2 = \mu^2 r^2(m) = \mu^2\left\{\frac{[\alpha + (\gamma+1)q(m)]}{\pi m} + \gamma\right\}, \tag{28}$$

where

$$m = \omega\eta n, \quad \alpha = \frac{\mathrm{E}\left[a_n^2\right]}{\mathrm{E}[a_n]^2}, \quad \gamma \equiv \frac{\mathrm{Cov}[a_r, a_s]}{\mathrm{E}[a_r]\mathrm{E}[a_s]} \quad (r \neq s)\,, \tag{29 -31}$$

$$q(m) = -1 + \frac{1}{2\pi m}[1 - \exp(-2\pi m)] + \mathrm{E}_1(\pi m)\left[\cosh(\pi m) - \frac{1}{\pi m}\sinh(\pi m)\right]. \tag{32}$$

Here m is the modal overlap factor, E_1 is the exponential integral, and the parameters α and γ can be calculated on the basis of the statistics of the applied loading and the (GOE) statistics of the mode shapes.

The variance of the slope of the kinetic energy has not previously been derived; it is shown in the Appendix that the following result can be found by using random point process theory in combination with GOE statistics:

$$\sigma_s^2 = \mu^2 n^2 \frac{\partial^2}{\partial m^2}\left[\frac{\alpha + (\gamma+1)q(m)}{\pi m}\right]. \tag{33}$$

If the modal overlap is greater than unity, then Eqs. (28) and (33) are well approximated by the simplified expressions

$$\sigma^2 \approx \mu^2\left\{\frac{(\alpha - \gamma - 1)}{\pi m} + \gamma\right\}, \quad \sigma_s^2 \approx \left(\frac{2}{\omega^2\eta^2}\right)\sigma^2\,, \tag{34,35}$$

where it should be noted that Eq. (35) is only valid for small γ. It follows from the equations in this section, together with Eq. (25), that the calculation of the mean rate of crossing the level b can be computed given only the system mass, modal density, and damping. The assumption of GOE statistics implies that the analysis is restricted to a system that that has non-localised modes, and this will typically mean a single structural component, but as discussed in Section 6 the method can be extended to built-up systems in a straight forward way.

3.3. The maximum crossing rate

It follows from Eqs. (10) and (25) that the crossing rate is a maximum when the exponent of the lognormal distribution of the kinetic energy is zero. The resulting maximum crossing rate is

$$\left(\nu_b^+\right)_{\max} = \beta\sigma_s\left[2\pi\mu^2\left(1 + \sigma^2/\mu^2\right)\ln\left(1 + \sigma^2/\mu^2\right)\right]^{-1/2}. \tag{36}$$

If the modal overlap of the system is sufficiently high (say $m > 2$) then the ratio σ/μ will be small, and with the adoption of the Gaussian value of β Eqs. (35) and (36) yield

$$\left(\nu_b^+\right)_{\max} \approx \frac{1}{2\pi}\left(\frac{\sqrt{2}}{\omega\eta}\right). \tag{37}$$

This result can be compared with that obtained for a stationary Gaussian random process [18].

$$\left(\nu_b^+\right)_{\max} \approx \frac{1}{2\pi}\left(\frac{\sigma_{\dot{y}}}{\sigma_y}\right). \tag{38}$$

In this case the maximum crossing rate occurs at $y = 0$, and $(\nu_b^+)_{\max}$ is interpreted as the mean frequency (in Hz) of the random process. This implies that $\sigma_{\dot{y}}/\sigma_y$ is the mean frequency of the random process when measured in rad/s. By analogy, the equivalent "circular frequency" of the kinetic energy is $\sqrt{2}/(\omega\eta)$; this quantity has units of time, and is similar to the quefrency used in cepstral analysis [26]. It is a curious fact that the result depends only on the modal bandwidth $\omega\eta$ and not on the modal density; it might initially be thought obvious that the mean "circular frequency" should be $2\pi n$, so that each mode is associated with an up-crossing, but this is clearly not the case. The fact that fluctuation rates are independent of the modal density has previously been noted in the literature: the quefrency $\sqrt{2}/(\omega\eta)$ is identically equal to the "mean rate of the phase rotation" derived by Schroeder for the pressure at a point in a room [1], and the parameter also fully determines the frequency autocorrelation function of the squared modulus of the pressure frequency response function [3]. The accuracy of Eq. (37) in the present context is considered in Section 5, where a comparison is made with numerical simulations.

3.4. Summary of the assumptions and approximations employed in the analysis

The key result of the foregoing analysis is Eq. (25), which gives the mean rate at which a random frequency response function crosses a level b with positive slope, and the three response parameters that appear in this result are detailed in

Eqs. (27), (28) and (33). A number of assumptions and approximations have been made in deriving Eq. (25), and these can be summarised as follows:

1) It has been assumed that the system has a sufficient degree of randomness for the natural frequencies and mode shapes to display GOE statistics (as noted in Section 3.2).
2) It has been assumed that the marginal distribution of the kinetic energy is lognormal, as shown in Eq. (10), which is a consequence of GOE statistics providing the modal overlap is not small [21].
3) On the basis of empirical evidence and the fact that $p(s|T)$ has analytical bounds that grow linearly with T, it has been assumed that the conditional standard deviation of s also grows linearly with T, as indicated in Eq. (20).
4) The conditional average value of s, for positive s, has been assumed to be proportional to the conditional standard deviation of s, as indicated in Eq. (24). This assumption is true if the conditional distribution of s is a single-parameter distribution, such as the Gaussian distribution or the exponential distribution, with the constant of proportionality depending on the distribution.
5) It has been assumed that s has zero mean, so that the kinetic energy has essentially been considered to be a stationary random process. This is generally not true, since the mean kinetic energy often varies with frequency; for example, if both the loss factor and the modal density are independent of frequency, then the mean kinetic energy will be inversely proportional to frequency [23]. In this case the assumption that s has zero mean can be rephrased as an assumption that the mean value of s is very small compared to the standard deviation. It can be shown from Eqs. (27), (34) and (35) that if the kinetic energy is inversely proportional to frequency then the mean value of s is of order $\eta\sqrt{m}\sigma_s$, which means that the assumption will be valid if $\eta\sqrt{m} << 1$. This conclusion can also be expected in more general cases.

The validity and accuracy of these assumptions is explored by comparison to numerical benchmark results in Section 5.

4. Other statistical properties

4.1. The probability of remaining below a critical level

The probability that a random process $y(t)$ will remain below a critical level in a given time interval has been much studied in the random vibration literature [18]; the results obtained in that field can be applied directly to the present work, where the interest is in the probability that a random frequency response function remains below a critical level b in a given frequency band. The simplest approach is to assume that up-crossings of the critical level constitute a Poisson point process, in which case the probability that the response will lie below b over the range $\omega_A \leq \omega \leq \omega_B$ can be written as [18].

$$P = P_0(b)\exp\left\{ -\int_{\omega_A}^{\omega_B} \nu_b^+(\omega)\mathrm{d}\omega \right\}, \tag{39}$$

where $P_0(b)$ is the probability that the response lies below b at $\omega = \omega_A$; this can be found by assuming a lognormal distribution of the energy at this frequency, in accordance with Eq. (10). If Eq. (39) is employed with the value $P_0(b) = 1$ then the equation has the alternative interpretation that it yields the probability that the level b will be neither up-crossed nor down-crossed, regardless of the initial conditions at $\omega = \omega_A$.

In the study of random vibration it has been found that the equivalent of Eq. (39) tends to underestimate P, and the result is therefore conservative from a safe-design viewpoint. The reason for the underestimation is that random vibrational crossings of a critical level tend to occur in "clumps", and this lowers the effective crossing rate [27]. Approximate methods of allowing for the occurrence of clumps are given in Ref. [28], while more sophisticated analysis methods based on the Fokker-Plank-Kolmogorov equation are described in Ref. [29]. In the present application it is not immediately clear if clumping will occur; on the contrary, mode repulsion might actually reduce the tendency for peaks in the frequency response function to occur near to each other, producing a form of "anti-clumping". Although issues of this type could in principle be explored analytically, it should be recalled that the present analysis is based on a number of approximations and assumptions, and building a more exact theory on this foundation is not thought to be appropriate. In this work Eq. (39) will be adopted, and the accuracy of the equation will be explored through numerical simulations in Section 5.

4.2. The average rate of occurrence of peaks

The frequency response function of the kinetic energy exhibits a peak every time the energy rate s crosses zero with negative derivative $\partial s/\partial\omega$. If the derivative of the energy rate is defined as r, so that

$$r(\omega) = \frac{\partial^2 T(\omega)}{\partial\omega^2}, \tag{40}$$

then the mean rate of occurrence of peaks can be expressed in terms of the joint probability density function $p(r,s)$ in form that is analogous to Eq. (9), i.e.

$$\nu_P = \int_{-\infty}^{0} |r| p(r,0) \mathrm{d}r. \tag{41}$$

Clearly the result will depend on the statistical distribution $p(r,s)$, which is not known in detail. The simplest way forward is to assume that the variables are Gaussian, zero mean, and uncorrelated, in which case Eq. (41) yields

$$\nu_P = \frac{1}{2\pi}\left(\frac{\sigma_r}{\sigma_s}\right), \tag{42}$$

where σ_r is the standard deviation of r, which is derived in the Appendix in the form

$$\sigma_r^2 = \mu^2 n^4 \frac{\partial^4}{\partial m^4}\left[\frac{\alpha + (\gamma+1)q(m)}{\pi m}\right]. \tag{43}$$

Equations (33), (42) and (43) can be combined to give an expression for the mean rate of occurrence of peaks, and if the modal overlap is greater than unity then it can readily be shown that

$$\nu_P \approx \frac{1}{2\pi}\left(\frac{\sqrt{12}}{\omega\eta}\right). \tag{44}$$

By comparing Eqs. (37) and (44) it can be seen that

$$\nu_P \Big/ \left(\nu_b^+\right)_{\max} \approx 2.44, \tag{45}$$

which means that the frequency response function of the energy is inherently broad-banded: on average there are more than two peaks for each up-crossing of the most crossed level, whereas the corresponding result for a narrow-banded process would be one peak per up-crossing. It is of interest to note from Eq. (45) that the extent to which the frequency response function is broad-banded is independent of the level of damping in the system, at least within the range of validity of the approximations employed in Eqs. (37) and (44).

Equation (44) can be compared to previous work by Schroeder by noting that in room acoustics the reverberation time can be written as $T_{60} = 4.4\pi/(\eta\omega)$, so that Eq. (44) can be re-expressed in the form

$$\nu_P \approx \frac{1}{2\pi}\left(\frac{3.99}{T_{60}}\right). \tag{46}$$

Equation (46) is in agreement with Eq. (13) of reference [2] which concerns the rate of occurrence of maxima in the modulus squared frequency response function of the pressure at a point in a room. Equation (42), together with Eqs. (33) and (43), represents a more general result, and the accuracy of this equation in the present context is explored via numerical simulations in Section 5.

4.3. The average trough-to-peak height

For a narrow-banded random process the statistical distribution of the peaks can be expressed in terms of the up-crossing rates [18]. It was shown in the previous subsection that the frequency response function of the energy is broad-banded, and so it is not possible to derive the distribution of the peaks in any simple way. However, one property that *can* be derived is the average value of the trough-to-peak height, and this can be done by noting initially that

$$\int_{\omega_A}^{\omega_B} |s| \mathrm{d}\omega \approx \sum_j |R_j|, \tag{47}$$

where R_j is the jth trough-to-peak height in the frequency response function over the range ω_A to ω_B, e.g. R_1 is the distance from the first peak to the first trough, R_2 is the distance from the first trough to the second peak, R_3 is the distance from the second peak to the second trough, and so on. It follows from Eq. (47) that the mean trough-to-peak height can be written in the form

$$\mathrm{E}[R] = \left[\frac{1}{2\nu_P(\omega_B - \omega_A)}\right] \int_{\omega_A}^{\omega_B} \mathrm{E}[|s|]\mathrm{d}\omega = \left(\frac{1}{2\nu_P}\right)\mathrm{E}[|s|]. \tag{48}$$

Taking s to be Gaussian, as in the previous sub-section, and noting Eq. (44), leads to the result

$$\mathrm{E}[R] = \sqrt{\pi/6}(\omega\eta\sigma_s). \tag{49}$$

Now if the approximation represented by Eq. (35) is adopted then

$$\mathrm{E}[R] = \sigma\sqrt{\pi/3} \approx 1.023\sigma, \tag{50}$$

which can be compared with the corresponding result for a narrow-band Gaussian random process [18], $\sigma\sqrt{2\pi} \approx 2.507\sigma$. Clearly the broad-banded nature of the frequency response function is associated with the occurrence of a number of low amplitude trough-to-peak cycles that reduce the average value of the fluctuations. The accuracy of Eq. (49) is explored in the following section via numerical simulations.

5. Numerical validations

In this section the accuracy of the foregoing theory is assessed by comparison with numerical results for a random plate. The plate considered is the same as that described in Section 2. To recap: the plate is simply supported and made of steel (Young's modulus $E = 2 \times 10^{11}\mathrm{N/m}^2$, density $\rho = 7800\,\mathrm{kg/m}^3$, and Poisson ratio $\nu = 0.3$) with thickness $h = 1\mathrm{mm}$ and planform dimensions $0.8\mathrm{m} \times 0.67\mathrm{m}$. Ten masses are attached in random positions, each having 2% of the mass of the bare plate. The response of the system has been calculated by using the Lagrange-Rayleigh-Ritz approach [19] employing the mode shapes of the bare plate as trial functions, and the kinetic energy in response to a point force of amplitude $\sqrt{2}$ N has been computed over the frequency range 2000 rad/s to 4000 rad/s. The modal density of the plate can be computed from the standard formula [24].

$$n = \left(\frac{A}{4\pi}\right)\left[\frac{12\rho(1-\nu^2)}{Eh^2}\right]^{1/2} = 0.0278 \ \ \mathrm{s/rad}, \tag{51}$$

where A is the planform area, giving approximately 55 modes over the frequency range of interest. A frequency dependent loss factor in the form $\eta = m/n\omega$ has been employed, so that the system has a constant specified value of the modal overlap factor m across the whole frequency range. An ensemble of 5000 systems has been considered in the numerical simulations.

The analytical predictions for the mean energy, the variance of the energy, and the variance of the energy rate, as given by Eqs. (27), (28) and (33), are compared with numerical simulations results in Figs. 5–7 respectively. In each case results are shown for four values of the modal overlap factor, $m = 1$, 2, 3, and 4. It can be noted that Eq. (27) requires the value of $\mathrm{E}[a_n]$ to be specified: for a point load a_n is equal to the square of the mode shape at the forcing point, and given that the modes are

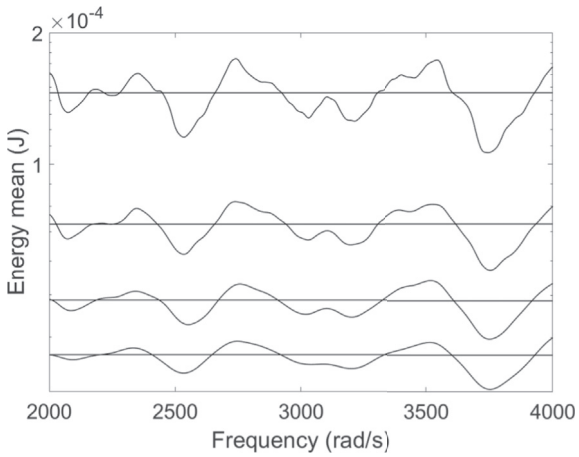

Fig. 5. The mean energy of a random plate plotted against frequency for four levels of damping (modal overlap). Straight lines: analytical predictions. Irregular curves: numerical simulations. The four values of modal overlap are $m = 1$, 2, 3, and 4, and these values yield decreasing values of the mean energy (i.e. the greatest results correspond to $m = 1$).

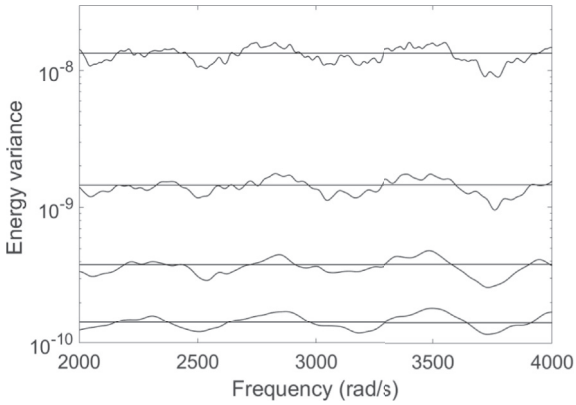

Fig. 6. The variance of the energy of a random plate plotted against frequency for four levels of damping (modal overlap). Straight lines: analytical predictions. Irregular curves: numerical simulations. The four values of modal overlap are $m = 1$, 2, 3, and 4, and these values yield decreasing values of the energy variance (i.e. the greatest results correspond to $m = 1$).

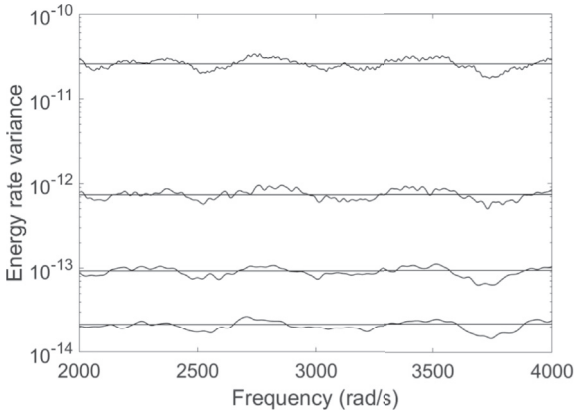

Fig. 7. The variance of the energy rate s (i.e. the frequency derivative of the energy) of a random plate plotted against frequency for four levels of damping (modal overlap). Straight lines: analytical predictions. Irregular curves: numerical simulations. The four values of modal overlap are $m = 1$, 2, 3, and 4, and these values yield decreasing values of the energy rate variance (i.e. the greatest results correspond to $m = 1$).

scaled to unit generalised mass the average value of this quantity is $1/M$, where M is the total mass of the plate. Likewise Eqs. (28) and (33) require the parameter α to be specified, as defined by Eq. (30). Were the mode shapes perfectly Gaussian, then the result would be $\alpha = 3$. Previous studies have found that in practice the value of α is less than this, and in the present work it has been found numerically that $\alpha = 2.85$. This is consistent with the fact that Brody et al. [30]. have shown that the occurrence of frame invariant GOE statistics in a system of finite size requires the mode shapes to be slightly non-Gaussian: the statistical moments of the mode shapes are given as a function the system size N in Eq. (7.13) of reference [30]. The value $\alpha = 2.85$ corresponds to $N = 38$, and this can be interpreted as the number of modes that interact and "mix" across the random ensemble. Equations (28) and (33) also employ the parameter γ which is defined by Eq. (31). The joint moments of the mode shapes can be calculated from Eq. (7.14) of reference [30] and for $N = 38$ this yields the value $\gamma = -0.05$. This value of γ, in conjunction with $\alpha = 2.85$, leads to the excellent predictions shown in Figs. 5–7.

The average number of up-crossings of a specified level b over the considered frequency range is shown as a function of b in Fig. 8, for four values of the modal overlap factor, $m = 1$, 2, 3, and 4. Two sets results are shown on each sub-plot: the continuous curve is the analytical result given by Eq. (25) using the "Gaussian" value of the parameter β, and the star symbols are the results yielded by the numerical simulations. The overall shape of the curves can be explained by reference to Fig. 1: the energy is positive definite, and so the rate of crossing the level $b = 0$ is zero; as the level is increased, the crossing rate increases to a maximum value, and then decreases to give a low rate of crossing very high levels. The overall level of agreement between the analytical predictions and the numerical simulations shown in Fig. 8 is considered to be very good, particularly when it is recalled that the present theory relies on a number of assumptions and approximations, as listed in Section 3.4. The most obvious assumption that might be questioned is that the system obeys GOE statistics. To explore the effect of this assumption, the numerical results for the case $m = 1$ have been recalculated by employing *exact* GOE statistics for the plate: the natural frequencies were generated from the eigenvalues of a GOE matrix [7], and the mode shapes were

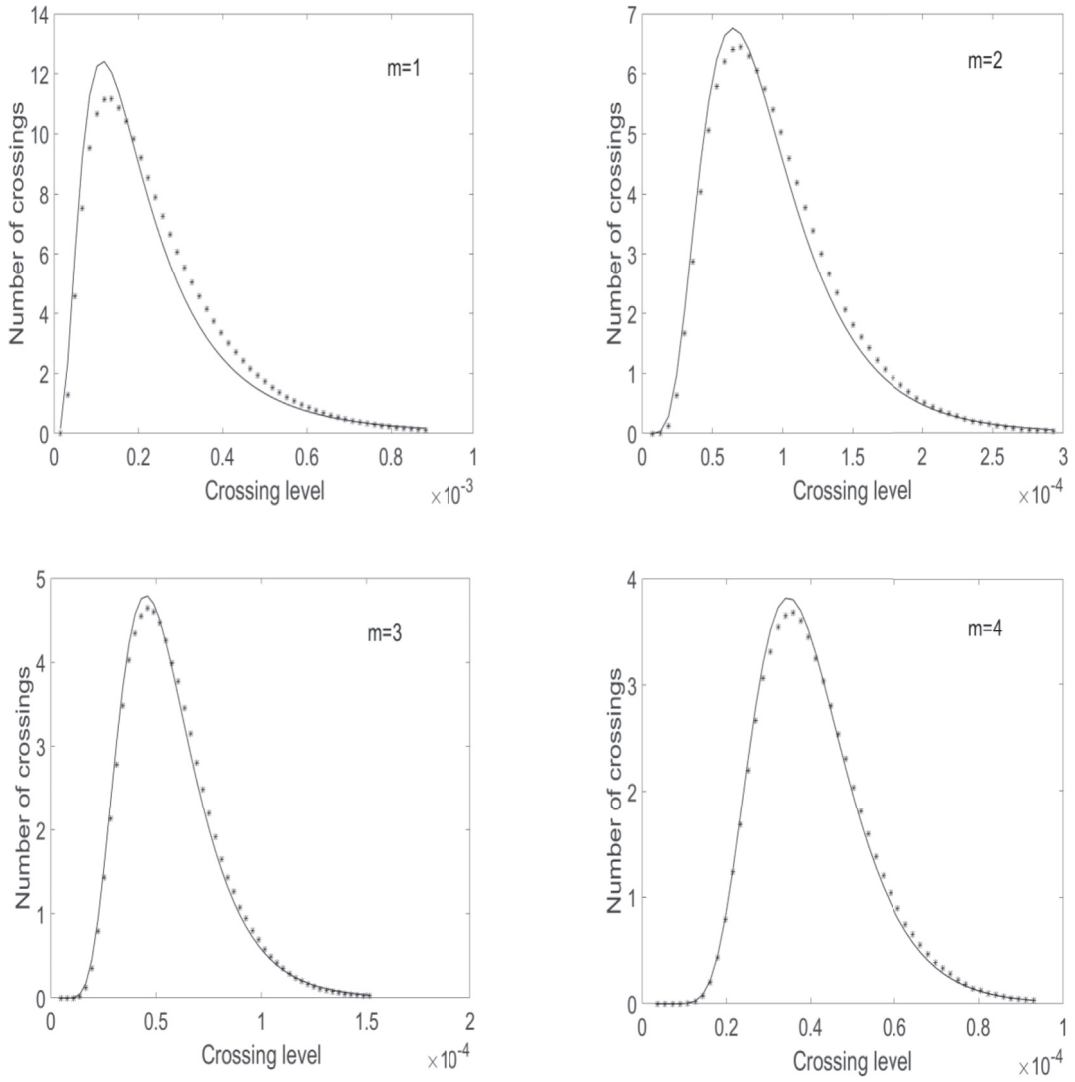

Fig. 8. The average number of up-crossings of the energy of a random plate over the frequency range 2000–4000 rad/s, plotted as a function of the crossing level b, for various values of the modal overlap factor m. Solid curves - analytical prediction; star symbols (*) - numerical simulations.

specified to be Gaussian and uncorrelated (the limit of the results given in Ref. [30] for a system of infinite size). The theoretical prediction to match this case has $\alpha = 3.0$ and $\gamma = 0$. The resulting numerical and analytical predictions are shown in Fig. 9, together with the previous results drawn from Fig. 8. It can be seem that the level of agreement between the analytical and numerical results is not improved by employing exact GOE statistics, suggesting that the mass loaded plate has GOE statistics to an adequate degree. The disagreements shown in Fig. 8 therefore stem from the other assumptions and approximations listed in Section 3.4; the development of a more sophisticated theory that would lift one or more of these assumptions would be extremely challenging, and it can be argued that the present theory yields good agreement in return for low analytical complexity.

The number of up-crossings of the most-crossed level is shown as a function of modal overlap in Fig. 10. These results correspond to the peaks of the curves shown in Fig. 8, and the corresponding results for a perfect GOE system are also shown. As found previously, the level of agreement between the analytical predictions and the numerical simulations is similar for the original system and the perfect GOE system. Also shown in the figure is a result calculated using the approximate maximum crossing rate given by Eq. (37). It can be seen that at high modal overlap this result approaches the perfect GOE results rather than the actual plate results, and this can be traced to the effect of modal correlations, as measured by γ. The effect of γ was ignored in Eq. (35) and hence in Eq. (37), and while this is valid for the perfect GOE system ($\gamma = 0$) it is not valid for the original system ($\gamma = -0.05$). It follows that the maximum crossing rate for the original system is best estimated from Eq. (36) rather than the more approximate result, Eq. (37).

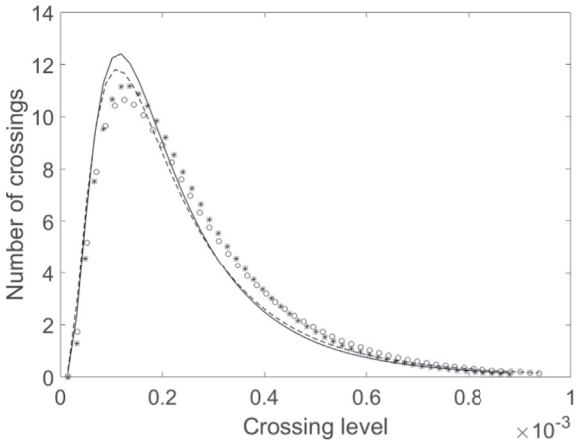

Fig. 9. The average number of up-crossings of the energy of a random plate over the frequency range 2000–4000 rad/s, plotted as a function of the crossing level b for the case $m = 1$. Solid curve - analytical prediction for a plate with random masses; star symbol (*) - numerical simulations for a plate with random mass attachements; dashed curve – analytical prediction for a plate with perfect GOE statistics; circle symbol (o) – numerical simulations for a plate with perfect GOE statistics.

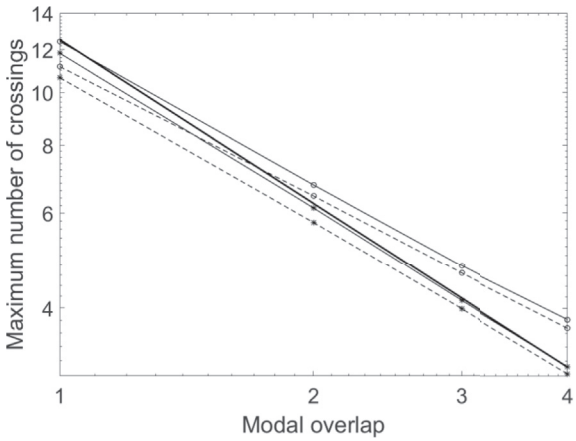

Fig. 10. The average number of up-crossings of the most crossed-level plotted as a function of the modal overlap. The results concern the energy of a random plate over the frequency range 2000–4000 rad/s. Light solid curves with symbols – analytical predictions; dashed curves with symbols – numerical simulations; circle symbol (o) – results for a plate with random mass attachments; star symbol (*) – results for a plate with perfect GOE statistics; heavy solid curve – prediction from Eq. (37).

Results for the probability of crossing a specified level b over the frequency range of interest are shown in Fig. 11 for the case $m = 2$. Here a "crossing" is defined as either a down-crossing or an up-crossing, so the system may lie (respectively) either above or below the specified level at the start of the frequency range. The analytical prediction of this probability is $1 - P$, where P is given by Eq. (39) with $P_0(b) = 1$. Three sets of results are shown in the figure: (i) the analytical predictions given by Eq. (39), (ii) the numerical results for the probability, and (iii) the results obtained by substituting the *numerical* result for the average crossing rate into Eq. (39). In the discussion below Eq. (39) it was noted that in random vibration the equation tends to underestimate P due to the phenomenon of clumping. An underestimation of P corresponds to an overestimation of $1 - P$, and in fact the reverse can be in seen in Fig. 11 if results (ii) and (iii) mentioned above are compared: Eq, (39) underestimates the probability of crossing the specified level. As mentioned in Section 4, this is due to the "anti-clumping" effect of mode repulsion, and this highlights a curious difference between the current application of crossing rate theory and the normal field of application. At high levels of b the predictions given by (ii) and (iii) agree, and this is consistent known results in random vibrations theory, where crossings of high levels are found to constitute a Poisson process, in which case Eq. (39) is exact. Turning to the fully analytical prediction yielded by Eqs. (25) and (39), it can be seen from the figure that reasonably good accuracy is obtained. The results at high levels of b are shown on a logarithmic scale in Fig. 12. If there is interest, for example, in the level that is crossed with a probability of 0.01, then the ratio of the analytical result to the numerical result is 1.17, representing a 17% error by this measure. This can be viewed as an acceptable error, given the approximate nature of the present theory and the complexity of the underlying problem. Results for the probability of

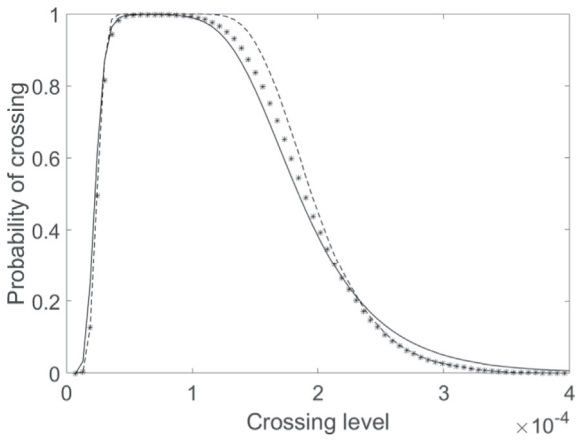

Fig. 11. Probability of crossing a specified level plotted as a function of the crossing level. The results concern the energy of a random plate over the frequency range 2000–4000 rad/s, with modal overlap $m = 2$. Solid curve – analytical predictions; dashed curve – numerical simulations; star symbols (*) – results obtained using Eq. (39) in combination with numerical simulation results for the crossing rate.

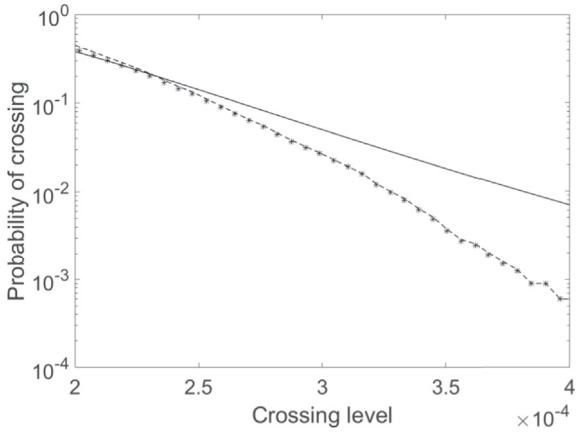

Fig. 12. A zoomed view of the results presented in Fig. 11.

crossing a specified level are shown in Figs. 13 and 14 for the case $m = 3$. The main trends are exactly as noted for Figs. 11 and 12, and in this case the error in predicting the level with a crossing probability of 0.01 is 8%.

The mean rate of occurrence of peaks is given by Eq. (42), and the maximum rate of up-crossing is given by Eq. (36); these two equations have been used to produce the results shown in Fig. 15 for the mean number of peaks per up-crossing. The theoretical predictions are shown as a function of the modal overlap factor for both the mass loaded plate and for the perfect GOE system, and in each case a comparison is made with numerical simulations. In general the agreement between the theoretical predictions and the numerical simulations is good, and the differences between the mass loaded plate and the perfect GOE system can be traced to the effect of γ, as in Fig. 10. Also shown in Fig. 15 is the constant value of 2.44 which is predicted by Eq. (45). This result agrees most closely with the results relating to the GOE system, and this is because the derivation of Eq. (45) employs Eq. (35), which neglects the influence of γ.

The mean trough-to-peak height, as predicted by Eq. (49), is shown in Fig. 16 as a function of the modal overlap factor. The results for both the mass loaded plate and the perfect GOE system are shown, and the results of the benchmark simulations are also plotted for each case. It can be seen that all of the results agree extremely closely, and this is partly because Eq. (49) depends only on σ_s and this parameter is very insensitive to the value of γ. Furthermore, the close agreement between the predictions and the numerical simulations justifies the assumptions that were made in the derivation of Eq. (49).

6. Conclusions

The main result of the present work is Eq. (25), which gives the mean crossing rate of the energy FRF of a random system in terms of the mean value of the function, the variance, and the variance of the frequency derivative. These three items can be evaluated on the basis of GOE statistics by using respectively Eqs. (27), (28) and (32), with Eq. (32) being a new result.

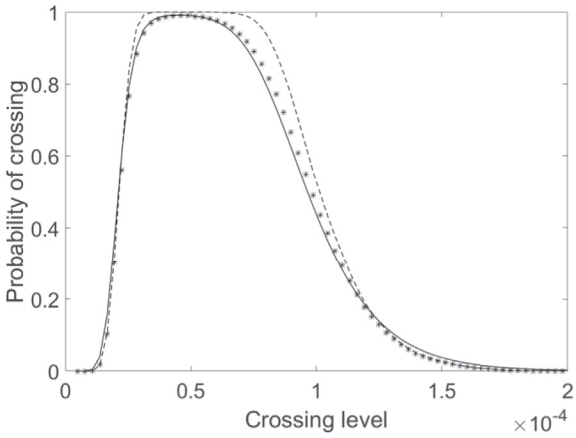

Fig. 13. Probability of crossing a specified level plotted as a function of the crossing level. The results concern the energy of a random plate over the frequency range 2000–4000 rad/s, with modal overlap $m = 3$. Solid curve – analytical predictions; dashed curve – numerical simulations; star symbols (*) – results obtained using Eq. (39) in combination with numerical simulation results for the crossing rate.

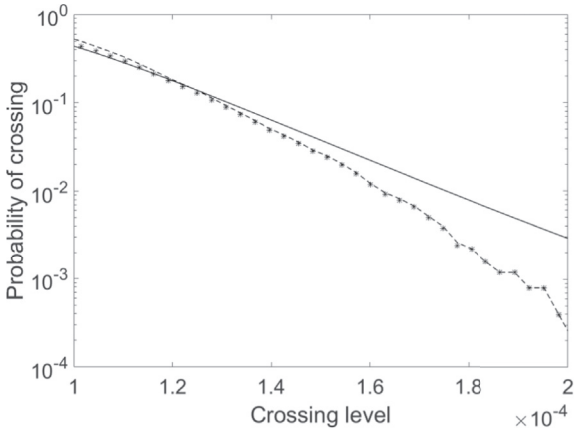

Fig. 14. A zoomed view of the results presented in Fig. 13.

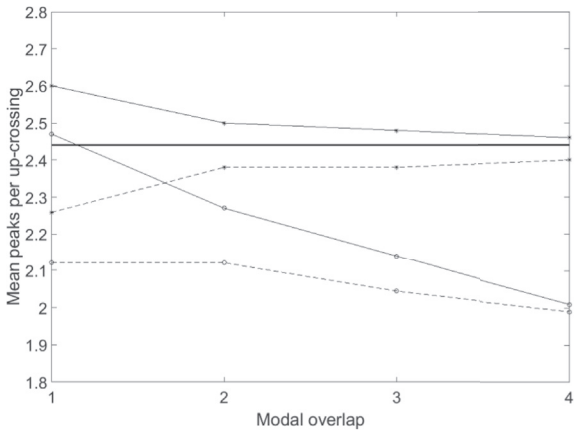

Fig. 15. The average number of peaks divided by the average number of up-crossings of the most crossed-level, plotted as a function of the modal overlap. The results concern the energy of a random plate over the frequency range 2000–4000 rad/s. Light solid curves with symbols – analytical predictions; dashed curves with symbols – numerical simulations; circle symbol (o) – results for a plate with random mass attachments; star symbol (*) – results for a plate with perfect GOE statistics; heavy solid curve – the approximation represented by Eq. (45).

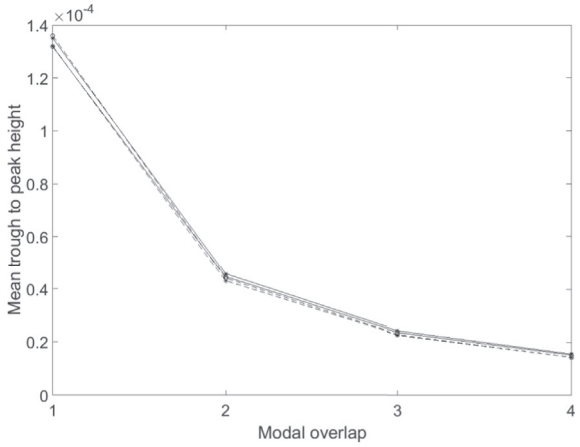

Fig. 16. The mean trough-to-peak height as a function of modal overlap. The curves are labelled as in Fig. 15.

The derivation of Eq. (25) involves a range of assumptions and approximations, and these are listed in Section 3.4; despite the seemingly restrictive nature of these assumptions, it has been found that Eq. (25) yields good accuracy for a mass loaded plate, and the same level of performance can be expected for any system that has global modes and has a sufficient degree of randomness (as defined in Section 3.2).

The probability of crossing a specified level within a given frequency range can be estimated from the crossing rate by using Eq. (39). Again, this equation has been found to show good accuracy when compared with numerical simulations. It has been found that in contrast to the case of random vibration, the equation tends to underestimate the probability of crossing a level, and physically this has been traced to an "anti-clumping" effect. In random vibration, crossings tend to occur in clumps, which reduces the effective rate of crossing, while in the present application mode repulsion reduces the tendency for peaks to occur in close proximity.

The mean rate of the occurrence of peaks has been derived in the form of Eq. (42), which leads to Eq. (44), and the mean trough-to-peak height is given by Eq. (49). Both of these results has been found to show good agreement with numerical simulations, which again justifies the underlying approximations and assumptions.

In the course of the analysis, three approximate "rules of thumb" have arisen: (i) the quefrency of the FRF is (approximately) independent of the modal density and is given by $\sqrt{2}/(\omega\eta)$, (ii) the number of peaks per up-crossing of the most crossed level is approximately 2.44, regardless of the level of damping, and (iii) the mean trough-to-peak height is approximately 1.02 times the standard deviation, in contrast to the value 2.507 that occurs for a Gaussian random process. It should be stressed that these results are approximations to the detailed values yielded by the present theory, but nonetheless they yield an interesting physical insight into the nature of the statistics of the FRF.

The present work has been restricted to a single structural component (or equivalently, a system having global modes). However, the results can readily be extended to a built-up system by following the approach taken in Ref. [13] – essentially the variance theory can be combined with Statistical Energy Analysis to compute the three parameters required by Eq. (25) for any subsystem of a complex system.

Acknowledgement

This work was funded in part through the EPSRC Research Grant EP/P005489/1 - SGRB64, Design by Science.

Appendix. derivation of the variance of the slope

It is shown in Ref. [25] that the variance of the kinetic energy described by Eq. (4) can be expressed in the form

$$\mathrm{Var}[T] = \mathrm{E}\left[a_n^2\right]\int_0^\infty [H(\omega,\omega_n)]^2 f_1(\omega_n)\mathrm{d}\omega_n + \mathrm{Cov}[a_n,a_m]\left\{\int_0^\infty H(\omega,\omega_n)f_1(\omega_n)\mathrm{d}\omega_n\right\}^2 + \Big\{\mathrm{Cov}[a_n,a_m] + \mathrm{E}[a_n]^2\Big\}\int_0^\infty\int_0^\infty H(\omega,\omega_n)H(\omega,\omega_m)g_2(\omega_n,\omega_m)\mathrm{d}\omega_n\mathrm{d}\omega_m, \tag{A1}$$

where $f_1(\omega)\equiv n(\omega)$ is the modal density of the system, and $g_2(\omega_n,\omega_m)$ is known as the correlation function or cluster function, arising from statistical correlations between the natural frequencies. This function is available in the GOE literature [7], and in

Ref. [11] the integrals in Eq. (A1) were evaluated to yield Eq. (28). For the present purposes it is helpful to re-express Eq. (A1) by introducing the Fourier transform of the function H in the form

$$h(\theta) = \int_{-\infty}^{\infty} H(\omega, \omega_n) e^{i\theta\omega_n} \mathrm{d}\omega_n, \quad H(\omega, \omega_n) = \left(\frac{1}{2\pi}\right) \int_{-\infty}^{\infty} h(\theta) e^{-i\theta\omega_n} \mathrm{d}\theta. \tag{A2),(A3}$$

When written in terms of $h(\theta)$ Eq. (A1) becomes

$$\begin{aligned} \mathrm{Var}[T] =& \mathrm{E}\left[a_n^2\right] \left(\frac{f_1}{2\pi}\right) \int_{-\infty}^{\infty} |h(\theta)|^2 \mathrm{d}\theta + \mathrm{Cov}[a_n, a_m] f_1^2 h^2(0) + \left\{\mathrm{Cov}[a_n, a_m] + \mathrm{E}[a_n]^2\right\} \\ & \left(\frac{1}{2\pi}\right)^2 \int_{-\infty}^{\infty} \int_{-\infty}^{\infty} h(\theta_1) h(\theta_2) G_2(-\theta_1, -\theta_2) \mathrm{d}\theta_1 \mathrm{d}\theta_2, \end{aligned} \tag{A4}$$

where

$$G_2(\theta_1, \theta_2) = \int_0^{\infty} \int_0^{\infty} g(\omega_n, \omega_m) e^{i\theta_1\omega_n} e^{i\theta_2\omega_m} \mathrm{d}\omega_n \mathrm{d}\omega_m. \tag{A5}$$

Now the value of the function $g_2(\omega_n, \omega_m)$ depends only on the difference frequency $\omega_n - \omega_m$, and this has the following implication regarding the form of the Fourier transform of the function:

$$g(\omega_n, \omega_m) = \widehat{g}(\omega_n - \omega_m) \quad \Rightarrow \quad G_2(\theta_1, \theta_2) = 2\pi \widehat{G}(\theta_1) \delta(\theta_1 + \theta_2) \tag{A6}$$

Here $\widehat{G}$ is the Fourier transform of $\widehat{g}$. Eqs. (A4) and (A6) imply that the variance of the kinetic energy can be expressed in the form

$$\mathrm{Var}[T] = \mathrm{E}\left[a_n^2\right] \left(\frac{f_1}{2\pi}\right) \int_{-\infty}^{\infty} |h(\theta)|^2 \mathrm{d}\theta + \mathrm{Cov}[a_n, a_m] f_1^2 h^2(0) + \left\{\mathrm{Cov}[a_n, a_m] + \mathrm{E}[a_n]^2\right\} \left(\frac{1}{2\pi}\right) \int_{-\infty}^{\infty} |h(\theta)|^2 \widehat{G}_2(-\theta) \mathrm{d}\theta. \tag{A7}$$

It follows from the discussion leading to Eq. (16) that the function $H(\omega, \omega_n)$ can be approximated as

$$H(\omega, \omega_n) \approx \frac{(1/4)}{4(\omega_n - \omega)^2 + (\eta\omega)^2}, \tag{A8}$$

which differs slightly from Eq. (16), but not in a material way, since the approximation is required to be accurate only in the region $\omega_n \approx \omega$. Eqs. (A2) and (A8) yield

$$h(\theta) = \left(\frac{\pi}{8\eta\omega}\right) \exp\left[-\left(\frac{1}{2}\right)\eta\omega|\theta| + i\omega\theta\right], \tag{A9}$$

and hence Eq. (A7) can be written in the form

$$\mathrm{Var}[T] = f_1^2 h^2(0) \left\{ \mathrm{E}\left[a_n^2\right] \left(\frac{1}{2\pi f_1}\right) \int_{-\infty}^{\infty} \mathrm{e}^{-\eta\omega|\theta|} \mathrm{d}\theta + \mathrm{Cov}[a_n, a_m] + \left(\mathrm{Cov}[a_n, a_m] + \mathrm{E}[a_n]^2\right) \left(\frac{1}{2\pi f_1^2}\right) \int_{-\infty}^{\infty} \mathrm{e}^{-\eta\omega|\theta|} \widehat{G}_2(-\theta) \mathrm{d}\theta \right\}. \tag{A10}$$

The term outside the curled brackets on the right of Eq. (A10) is the square of the mean response [23], and hence the equation can be rewritten as

$$\mathrm{Var}[T] = \mathrm{E}[T]^2 r^2(m), \tag{A11}$$

where $r^2(m)$ is the term inside the curled brackets, which corresponds to the relative variance of the energy.

The above analysis has been concerned with the variance of the energy, whereas the ultimate aim of this Appendix to derive an expression for the variance of the derivative of the energy. This can be done by replacing $H(\omega, \omega_n)$ by its frequency derivative throughout the analysis, In particular, the Fourier transform is modified as follows

$$\int_{-\infty}^{\infty} \frac{\partial H(\omega,\omega_n)}{\partial \omega} e^{i\theta\omega_n} \mathrm{d}\omega_n \approx -\int_{-\infty}^{\infty} \frac{\partial H(\omega,\omega_n)}{\partial \omega_n} e^{i\theta\omega_n} \mathrm{d}\omega_n = i\theta h(\theta). \tag{A12}$$

By replacing $h(\theta)$ in Eq. (A7) with $i\theta h(\theta)$ it follows immediately that

$$\mathrm{Var}\left[\frac{\partial T}{\partial \omega}\right] = f_1^2 h^2(0)\left\{ \mathrm{E}\left[a_n^2\right]\left(\frac{1}{2\pi f_1}\right)\int_{-\infty}^{\infty} \theta^2 \mathrm{e}^{-\eta\omega|\theta|}\mathrm{d}\theta + \left(\mathrm{Cov}[a_n,a_m] + \mathrm{E}[a_n]^2\right)\left(\frac{1}{2\pi f_1^2}\right)\int_{-\infty}^{\infty} \theta^2 \mathrm{e}^{-\eta\omega|\theta|}\widehat{G}_2(-\theta)\mathrm{d}\theta \right\}. \tag{A13}$$

By comparing this result with Eqs. (A10) and (A11) it can be seen that

$$\mathrm{Var}\left[\frac{\partial T}{\partial \omega}\right] = \mathrm{E}[T]^2 \frac{\partial^2}{\partial(\omega\eta)^2}\left[r^2(m)\right] = \mathrm{E}[T]^2 f_1^2 \frac{\partial^2}{\partial m^2}\left[r^2(m)\right]. \tag{A14}$$

This result leads immediately to Eq. (33) in Section 3.2.

If the second derivative of the kinetic energy is of concern, then the right hand side of the equivalent of Eq. (A12) is $-\theta^2 h(\theta)$, and following through the subsequent analysis leads immediately to the result

$$\mathrm{Var}\left[\frac{\partial^2 T}{\partial \omega^2}\right] = \mathrm{E}[T]^2 f_1^4 \frac{\partial^4}{\partial m^4}\left[r^2(m)\right]. \tag{A15}$$

References

[1] M.R. Schroeder, Die Statistischen parameter der frequenzkurven von grossen raumen, Acustica (1954) 594–600.
[2] M.R. Schroeder, K.H. Kuttruff, On frequency response curves in rooms, comparison of experimental, theoretical, and Monte Carlo results for the average spacing between maxima, J. Acoust. Soc. Am. 34 (1962) 76–80.
[3] M.R. Schroeder, Frequency-correlation functions of frequency responses in rooms, J. Acoust. Soc. Am. 34 (1962) 1819–1823.
[4] R.H. Lyon, Statistical analysis of power injection and response in structures and rooms, J. Acoust. Soc. Am. 45 (1969) 545–565.
[5] R.H. Lyon, Progressive phase trends in multi-degree-of-freedom systems, J. Acoust. Soc. Am. 73 (1983) 1223–1228.
[6] M. Tohyama, R.H. Lyon, T. Koike, Reverberant phase in a room and zeros in the complex frequency plane, J. Acoust. Soc. Am. 89 (1991) 1701–1707.
[7] M.L. Mehta, Random Matrices, second ed., Academic Press, San Diego, 1991.
[8] R.L. Weaver, Spectral statistics in elastodynamics, J. Acoust. Soc. Am. 85 (1989) 1005–1013.
[9] R.L. Weaver, The unreasonable effectiveness of random matrix theory for the vibrations and acoustics of complex structures, in: M.C.M. Wright, R. Weaver (Eds.), New Directions in Linear Acoustics and Vibration: Quantum Chaos, Random Matrix Theory, and Complexity, Cambridge University Press, Cambridge, 2010.
[10] O.I. Lobkis, R.L. Weaver, I. Rozhkov, Power variances and decay curvature in a reverberant system, J. Sound. Vib. 237 (2000) 281–302.
[11] R.S. Langley, A.W.M. Brown, The ensemble statistics of the energy of a random system subjected to harmonic excitation, J. Sound. Vib. 275 (2004) 823–846.
[12] R.S. Langley, A.W.M. Brown, The ensemble statistics of the band-averaged energy of a random system, J. Sound. Vib. 275 (2004) 847–857.
[13] R.S. Langley, V. Cotoni, Response variance prediction in the statistical energy analysis of built-up systems, J. Acoust. Soc. Am. 115 (2004) 706–718.
[14] R.S. Langley, V. Cotoni, Response variance prediction for uncertain vibro-acoustic systems using a hybrid deterministic-statistical method, J. Acoust. Soc. Am. 122 (2007) 3445–3463.
[15] A.J. Keane, P.B. Nair, Computational Approaches for Aerospace Design, John Wiley and Sons, Hoboken, 2005.
[16] C. Soize, A comprehensive overview of a non-parametric probabilistic approach of model uncertainties for predictive models in structural dynamics, J. Sound. Vib. 288 (2005) 623–652.
[17] V. Cotoni, R.S. Langley, M.R.F. Kidner, Numerical and experimental validation of variance prediction in the statistical energy analysis of built-up systems, J. Sound. Vib. 288 (2005) 701–728.
[18] Y.K. Lin, Probabilistic Theory of Structural Dynamics, McGraw-Hill, New York, 1967.
[19] L. Meirovitch, Elements of Vibration Analysis, second ed., McGraw Hill, New York, 1986.
[20] S.O. Rice, Mathematical analysis of random noise, in: N. Wax (Ed.), Selected Papers on Noise and Stochastic Processes, Dover Publications, New York, 1954.
[21] R.S. Langley, J. Legault, J. Woodhouse, E. Reynders, On the applicability of the lognormal distribution in random dynamical systems, J. Sound. Vib. 332 (2013) 3289–3302.
[22] N.J. Kessissoglou, G.I. Lucas, Gaussian orthogonal ensemble spacing statistics and the statistical overlap factor applied to dynamic systems, J. Sound. Vib. 324 (2009) 1039–1066.
[23] R.S. Langley, The analysis of random built-up engineering systems, in: M.C.M. Wright, R. Weaver (Eds.), New Directions in Linear Acoustics and Vibration: Quantum Chaos, Random Matrix Theory, and Complexity, Cambridge University Press, Cambridge, 2010.
[24] L. Cremer, M. Heckl, E.E. Ungar, Structure-borne Sound, Springer, Berlin, 1988.
[25] R.S. Langley, A. Cicirello, E. Deckers, The ensemble statistics of the energy of a harmonically excited random system, J. Sound. Vib. (2017) in press.
[26] R.B. Randall, Frequency Analysis, Bruel and Kjaer, Naerum, 1987.
[27] E.H. Vanmarcke, On the distribution of the first-passage time for normal stationary random processes, J. Appl. Mech. 42 (1975) 215–220.
[28] N.C. Nigam, Introduction to Random Vibrations, MIT Press, Cambridge MA, 1983.
[29] R.S. Langley, A variational formulation of the FPK equations with application to the first passage problem in random vibration, J. Sound. Vib. 123 (1988) 213–227.
[30] T.A. Brody, J. Flores, J.B. French, P.A. Mello, A. Pandey, S.S.M. Wong, Random-matrix physics: spectrum and strength fluctuations, Rev. Mod. Phys. 53 (1981) 385–479.